Direct Probing of Electrical Double Layers by Scanning Electrochemical Potential Microscopy

Cedric Hurth,[†] Chunzeng Li,[‡] and Allen J. Bard*,[†]

Department of Chemistry and Biochemistry, The University of Texas at Austin, Austin, Texas 78712, and Veeco Instruments, Santa Barbara, California 93117

We report the direct experimental measurement of electrical double layer profiles on metallic (Pt foil) and insulator (SiO_2 on Si) surfaces in a dilute electrolyte with no added redox mediator by scanning electrochemical potential microscopy (SECPM). An important consideration in these measurements is fabrication of the probe (tip), and experimental details are given for the reproducible preparation of suitable polyethylene-coated PtIr nanoelectrodes. A small amount of silver was electrodeposited on these tips to stabilize them for sensitive potentiometric measurements. A Pt foil surface and an oxide-grown Si(100) wafer in 10 μM KCl were approached to record the potential distribution in the vicinity of the surface. The advantages and limitations of SECPM are compared to conventional current-sensing techniques.

Introduction

The measurement of charge distributions near the surfaces of conductors and insulators immersed in liquids, desirably with ~1 Å resolution, could provide useful information about local electric fields and ionic concentrations. For example, by studying the potential as a function of distance near a surface in a solution of known ionic strength, one could map the electrical double layer (EDL) and test the various numerical[1] or analytical[2,3] approaches to Gouy−Chapman−Stern and Derjaguin−Landau−Overbeek (DLVO) theory. Relevant experimental data for this is most frequently obtained by measuring the double-layer capacitance with impedance techniques[14] or the zeta potential by streaming potential techniques.[4] The variety of scanning probe techniques that have been developed since the introduction of scanning tunneling microscopy (STM) in 1982[5] allows one to access various local properties of solid surfaces. For example, the study of EDLs has been carried out with atomic force microscopy (AFM)[6,7] or by scanning surface potential microscopy[8] by measuring surface forces in a modification of the technique using crossed mica cylinders to obtain information on the forces between charged surfaces.[9] However, the AFM probes used in these studies must be modified with large, micrometer-sized, silica spheres to obtain a sufficient force for measurement as well as a geometry for easy comparison with the available DLVO treatment. This probe modification results in loss of potential control as the silica surface charge can only be controlled indirectly by the ionic strength or the solution pH[10] within certain limits. Additionally, the attractive van der Waals contribution needs to be calculated and subtracted from the measured force, which provides a potential source of error.

Scanning Kelvin probe microscopy[11] is another potentially fruitful technique to measure surface potentials. However, its application is limited to the gas phase because the large tip potentials involved would result in large faradaic processes. Electric force microscopy (EFM)[12] measures the electric force between a conductive tip and the sample, typically with a dc bias voltage applied to enhance the signal. Again, there is no separation between the van der Waals and the electrostatic contributions to the measured resulting capacitive force between the tip (attached to the cantilever) and the sample in both of these local techniques.

Recently, the direct measurement of the electrostatic contribution in the DLVO theory to study electrode/electrolyte interfaces has been reported[13] in an approach close to what is described in this paper. The home-built instrument and the metallic probes used were largely inspired by extensive previous work on tunneling microscopy in an electrolytic environment (EC-STM). The gold probe was at open circuit, and its potential was fed into a high input impedance voltage follower. The major assumption is that the probe does not perturb the surface double layer and reads the potential directly, i.e., without passing current.

The EDL is important in electrochemistry and colloid science. Its detailed structure and modification upon interfacial changes have been the focus of decades of theoretical and experimental research[14] since 1923, when Gouy, Chapman, and Stern proposed their description of the double layer extending Helmholtz's early observations.[15] The model describes the one-dimensional potential distribution at a charged metallic surface quite well but fails to take into account finer interfacial effects arising when, for instance, two double layers overlap, i.e., when co-ions and counterions no longer obey the Boltzmann distribution[16] because of confinement or when surface roughness cannot be neglected.[17] The DLVO theory has been used most extensively to interpret experimental results from electrolytes and surfactants,[18] polymers,[19] or proteins[20] because it proposes a quite complete treatment including contributions from dispersive and electrostatic interactions as well as from interfacial solvent molecules.

We describe here experiments with a new technique, scanning electrochemical potential microscopy (SECPM),[21] to investigate the potential distribution in the nanogap formed between several surfaces, including Pt and Si/SiO$_2$, and a metal probe tip. In SECPM, the tip is held at open circuit with a high impedance amplifier, while the surface, if conducting, is maintained at a

Electrochemical Potential Microscopy

J. Phys. Chem. C, Vol. 111, No. 12, 2007 **4621**
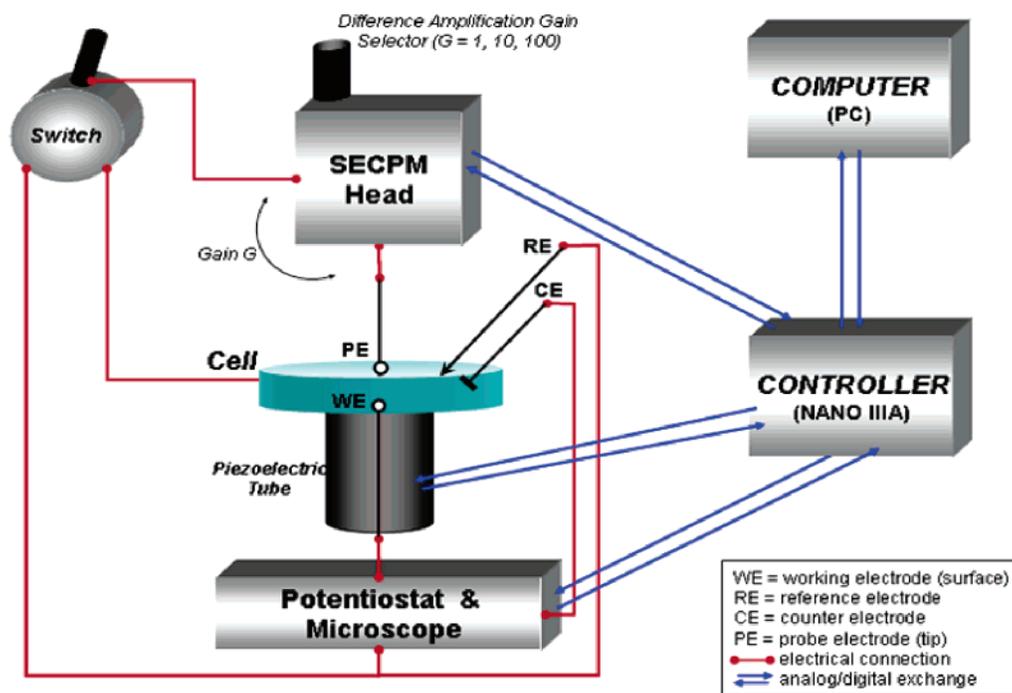
Figure 1. Simplified block diagram for SECPM. The open-circuit potential of the tip is measured and fed into a high impedance amplifier. A manual switch was added to allow measuring of the potential with respect to the surface potential as well as a stable reference electrode.

specified potential in a three-electrode cell system connected to a potentiostat. The tip potential is measured with respect to a stable reference electrode (or optionally with respect to the substrate). A block diagram is given in Figure 1.

Experimental Section

SECPM Probe Preparation. An important factor in a successful SECPM experiment is the tip. It is difficult to have an unpoised inert electrode, e.g., Pt, i.e., an electrode whose potential is not governed by a redox equilibrium that will maintain a stable potential with time. For example, the potential of a Pt electrode immersed in an electrolyte not containing any purposely added reversible redox couple should technically be at the potential of zero charge, but in fact its potential is often governed by adventitious impurities, trace oxygen, and other species that can undergo charge exchange reactions at the electrode. Simply following the evolution of the open-circuit potential of a large Pt electrode (>6 mm^2) in a dilute aqueous solution of a symmetric electrolyte shows that the potential cannot be poised at a stable predictable value. The residual oxygen content even after deaeration and the presence of redox active impurities are among factors that affect the open-circuit potential of the electrode when the electrolyte does not contain a redox species at an appreciable concentration. Metals like Hg or Ag tend to show more stable behavior, since they are less electrocatalytic for processes like oxygen and proton reduction, but the potential still tends to drift.

Probe Insulation. It is also necessary to make the metallic electrode as small as possible by insulating all but the apex with an insulating chemically inert coating to obtain the required spatial resolution within the double layer. The maximum extension of the exposed metallic electrode protruding from the insulating sheath must be much smaller than the expected Debye length of the diffuse double layer. A 0.25 mm diameter $Pt_{0.8}$-$Ir_{0.2}$ wire (Sigma Aldrich) was etched in a saturated 60% (w/w) $CaCl_2$ solution with 4% (w/w) HCl by applying 35 V ac at 60 Hz to form a sharp tapered protrusion near the air/electrolyte

interface.[22] Low-density polyethylene (LDPE), used commercially in glue guns, was employed to insulate such etched tips. At about 170 °C, the viscosity of the glue allowed covering of a sharp tip without exposing its apex. The coating thus forms a thin layer around the etched Pt wire similar to that of a previously reported method using Apiezon wax.[23] The polyethylene coating was then made thinner at the tip apex by locally heating the polymer layer under an optical microscope. The LDPE layer was inert in a concentrated 1 M sulfuric acid solution for at least several hours, since no alteration of the capacitive voltammogram could be observed. The coating was also relatively stable in 1 M nitric acid for an hour. Voltammograms in 1 M H_2SO_4 at high scan rates (1.7 V/s) gave an approximate average coating thickness of about 200 nm at the apex when the coating layer was modeled as a resistor and a capacitor in parallel (Figure 2).

Tip Apex Exposure. The end of an insulated electrode was exposed by approaching a Pt foil surface (99.99%, Sigma Aldrich, exposed area 0.2 cm^2) within the tunneling regime in a dilute 10 μM KCl or KF electrolyte with the purpose of making a hole in the thinned polyethylene coating at the apex.[24] The Pt foil was ultrasonicated in methanol and Milli-Q water (18 MΩ·cm), immersed in a solution made from equal volumes of 30% (w/w) H_2O_2 and 0.1 M H_2SO_4, and thoroughly rinsed with Milli-Q water before each experiment. A bias of $+800$ mV was applied between the tip (at $+600$ mV vs a platinum$-$polypyrrole (PtPPy) reference electrode[25]) and the surface (at -200 mV). Initially, far from the surface, the measured tip current was within the noise level (±20 pA). The feedback loop on the tip current was set to $+150$ pA, and the integral and proportional gains were set to large values (~5) to trigger a fast response to a sudden change in the tip current. A current of 150 ± 40 pA was produced when the tip "touched" the Pt foil and was allowed to flow for about 5 s. The higher noise level observed under this condition is attributed to the additional faradaic current from water oxidation that flows at such positive
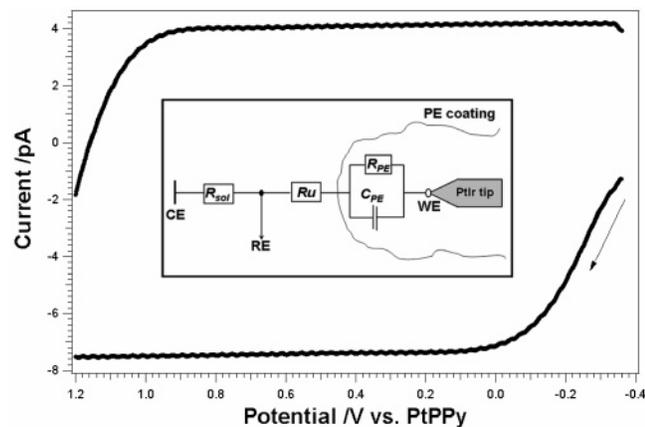
Figure 2. Cyclic voltammogram of a thinned polyethylene coated, etched PtIr tip in 1 M sulfuric acid. The potential is swept from −360 mV vs PtPPy (10 s quiet time) to 1.3 V vs PtPPy at 1.7 V/s. A low-pass second-order filter with a cutoff frequency of 1.5 Hz and a grounded Faraday cage were used in recording the data. The inset shows the model circuit used to determine an approximate coating thickness of 200 nm at the apex. Key to figure: R_{sol}, solution resistance; R_u, uncompensated resistance; R_{PE}, polyethylene (PE) leakage resistance; C_{PE}, polyethylene (PE) capacitance; WE, working electrode (PtIr tip); RE, reference electrode; CE, counter electrode (Pt wire).

overpotentials and creates a negative current that opposes the tunneling current.

The tip was then withdrawn 20 μm from the surface by the stepper motor where the current dropped back to within the instrument noise level (no dependence on applied potential). A rough Pt foil surface was preferred over evaporated gold on mica or highly oriented pyrolytic graphite because only in the case of Pt was the leakage current of the tip identical before and after the tunneling current was observed, suggesting that no significant amount of material was irreversibly transferred from the surface to the tip. At this point, a cyclic voltammogram (CV) in 1 M H_2SO_4 was taken at 1.7 V/s to estimate the cleanliness and exposed area of the Pt electrode. The voltammograms reproducibly showed broadened unresolved hydrogen adsorption/desorption peaks, followed by a shortened double-layer region and a large oxide formation region attributed to dissolved oxygen in a nondeaerated solution. The current in the double-layer region was typically between 4 and 60 pA.

Cyclic voltammetry of a well-defined disk ultramicroelectrode (UME) consisting of a 25 μm diameter Pt wire embedded in an insulating borosilicate glass layer (2 mm diameter) at a series of scan rates from 10 mV/s to 1.7 V/s was carried out in the same 1 M H_2SO_4 solution. The measured capacitance in the double-layer region of the voltammogram could not be used to estimate the area, since the measurement was perturbed by stray capacitance even when the cell was placed in the Faraday cage. Therefore, the PtO reduction peak was used. For a 25 μm diameter disk, the charge from the area under the peak during the PO reduction process was 27.7 nC. The same measurement showed typically 64 pC for the LDPE-insulated SECPM tips (Figure 4). Therefore, with the use of the linear dependence of the charge with the electrode area in the hemisphere approximation, the SECPM PtIr tips were found to have a radius of about 400 nm.

The possibility of the LDPE coating totally resealing the exposed Pt apex due to its higher elasticity compared with Apiezon wax once the tip is withdrawn from the surface is tempered by the small current and nondistorted shape of the voltammogram in sulfuric acid obtained immediately after the

opening sequence. When the probe that was opened by the tunneling process was used immediately to image the Pt foil surface in a dilute KF or KCl solution (Figure 3), the observed roughness was consistent with the roughness measured by tapping-mode AFM (data not shown), suggesting that the Pt electrode was protruding or only slightly recessed within the LDPE coating, or otherwise the vertical contrast obtained in the constant height image in a noncorrosive electrolyte would largely differ from the topography image obtained by AFM. Additionally, scanning electron microscopy of such a probe with a low-energy electron beam necessary to preserve the LDPE coating showed a large flattened area ($\sim$1 μm^2) from mechanical contact with the Pt surface in the opening procedure but no metallic protrusion clearly visible from the surrounding bright LDPE coating charged by the electron beam. The hypothesis of a mechanical contact between the insulated tip and the metallic surface was strengthened by the EC-STM image since a crater—about 5 nm deeper than the average surface plane— can be seen on the bottom left part of the image (Figure 3). At this point, we believe the dielectric coating breaks down due to the applied high electric field, and the Pt electrode was then subsequently slightly pushed into the polyethylene coating compressed by the contact with the Pt foil surface.

Metal Electrodeposition. With a Pt or Au electrode and an electrolyte such as KF or $NaBF_4$,[13] which show no specific adsorption,[26,27] a stable tip potential at open circuit was not obtained, as discussed earlier. For better stabilization we tried plating either Hg or Ag on the PtIr tip. Hg was deposited onto opened PtIr probes from a 10 μM $Hg_2(NO_3)_2$, 0.1 M KNO_3, and 0.5% HNO_3 solution electrolytically; this should decrease the sensitivity to dissolved oxygen and extend the potential region where only double-layer charging occurs compared with a bare Pt electrode. The Hg content in the plating solution was decreased compared with those of usual procedures to form stable Hg drops or films on Pt UMEs[28] because of the expected sub-micrometer dimensions of the Pt electrodes. Hg could be reproducibly deposited on the Pt electrodes[29] and formed a uniform coating according to CV in 1 M sulfuric acid, but the Hg film would not last over an extended series (several tens) of approach curves to the Pt electrode as shown in the comparison of cyclic voltammograms in 1 M H_2SO_4 before and after a series of approach/retract cycles in the potentiometry mode.

Silver was electrodeposited onto a freshly opened insulated Pt probe from a 36 g/L AgCN solution containing 60 g/L KCN and 45 g/L K_2CO_3[30] for experiments in dilute KCl to stabilize the potential of the Ag electrode by the specific anionic adsorption and strong interaction of Cl[31] and to map the potential profiles in these solutions.

Tip Characterization. Characterization of exposed Pt tips by linear sweep voltammetry in 0.1 M $Ru(NH_3)_6^{3+}$ solution in 100 mM pH = 7 phosphate buffer or a 100 mM $K_4Fe(CN)_6$ solution with 0.1 M KCl often showed a distorted curve from the expected steady-state sigmoidal behavior, suggesting electrolyte leakage between the coating and the Pt or a complex recessed electrode geometry. Upon deposition of Ag, the potential shifted to a more positive value corresponding to the expected half-wave potential for ruthenium hexamine and recovered its sigmoidal shape. Additionally, the voltammogram of a PtIr probe electrodeposited with silver in a 1 M sulfuric acid solution was recorded after the opening sequence in the tunneling microscope and immediately after the silver deposition to estimate the coverage efficiency of the Pt electrode by the silver film (Figure 4).

Electrochemical Potential Microscopy

J. Phys. Chem. C, Vol. 111, No. 12, 2007 **4623**
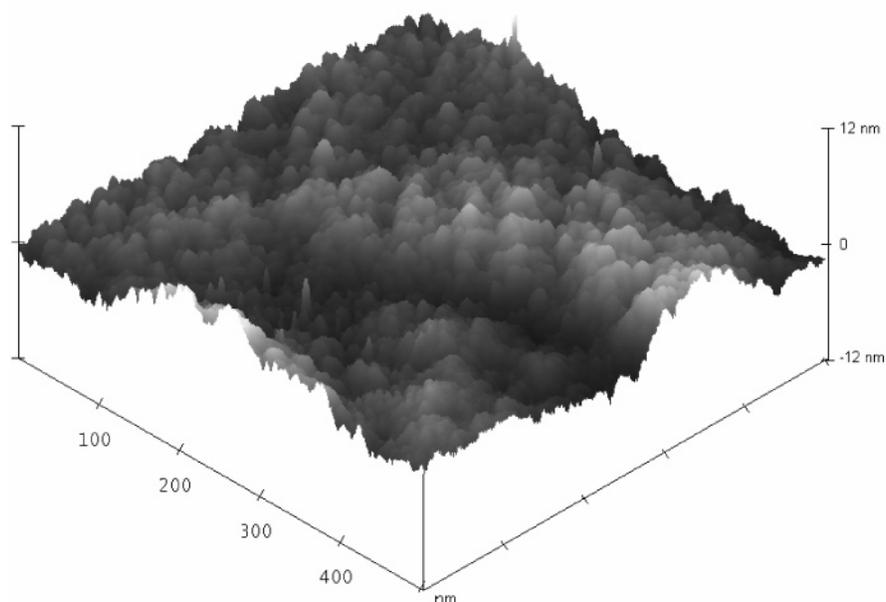
Figure 3. EC-STM image of the Pt foil surface obtained in 10 μM KF immediately after the opening sequence with a tip bias of +600 mV and a setpoint current of 150 pA. A 200 nm wide crater can be seen in the bottom left corner of the image and could be the result of a mechanical contact contributing to the tip opening. The roughness (R_q = 1.35 nm (excluding the crater)) is consistent with that obtained from an ex situ tapping-mode AFM scan of the same Pt foil surface (R_q = 1.14 nm). The AFM images are flattened line-by-line with a second-order polynomial to remove tilt and artifacts, such as bow in the scan.
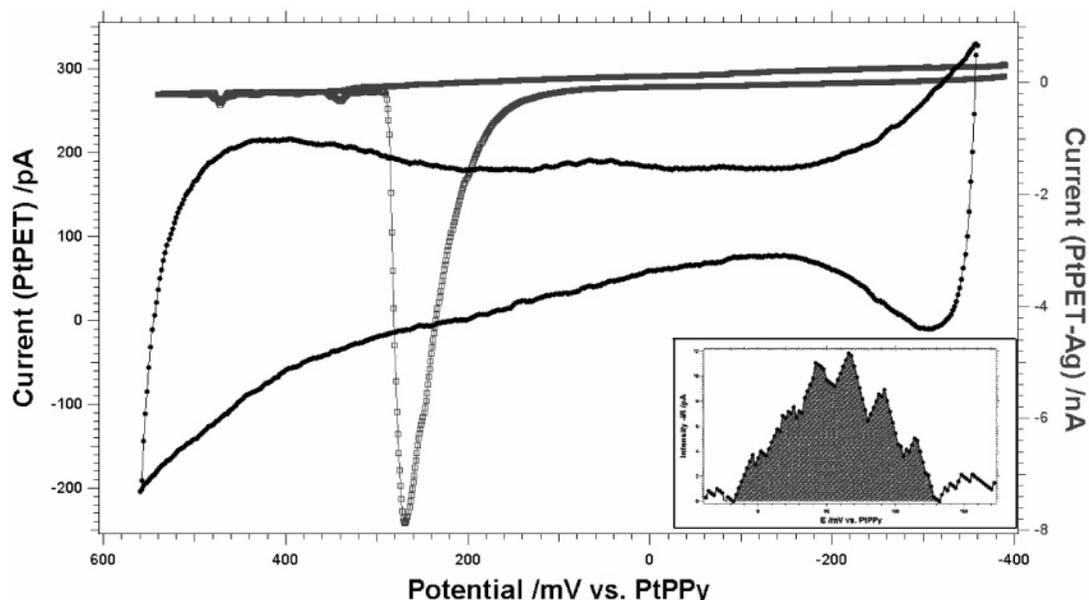
Figure 4. Cyclic voltammogram of an STM-opened PtIr tip in 1 M sulfuric acid at 1.7 V/s before (filled black circles) and after (empty gray squares) Ag deposition from a 0.2 M AgCN solution. A low-pass second-order filter with a cutoff frequency of 1.5 Hz and a grounded Faraday cage were used in recording the data. A large amount of Ag strips from the probe and no hydrogen adsorption/desorption peaks can be distinguished. This suggests an extensive coverage of the Pt electrode underneath. The inset shows a magnification of the area corresponding to the reduction of the surface Pt oxide used to determine the size of the electrode.

Chemicals and Apparatus. CaCl$_2$, KF, KCl, KNO$_3$, KCN, K$_2$CO$_3$, Hg$_2$(NO$_3$)$_2$·2H$_2$O, AgCN, and Ru(NH$_3$)$_6$Cl$_2$ were purchased as solids at the highest available purity. Hygroscopic salts were stored in a desiccator. H$_2$SO$_4$, HNO$_3$, HF, or HCl solutions were prepared by diluting concentrated solutions obtained at the analytical grade from Fisher Scientific. Pt$_{80}$Ir$_{20}$ wires used to prepare the tips were purchased as drawn at 99.99% purity from Goodfellow Corporation. Pt wires to prepare the PtPPy reference electrode and the counter electrode were purchased in 99.99% annealed reels from Goodfellow Corporation. All wires were immersed in concentrated

or 1 M HNO$_3$ prior to use. The electrochemical cells were homemade from Teflon, cleaned in (70:30) Piranha solution heated at 80 °C for 30 min, and ultrasonicated in methanol and then purified water before use. All solutions were made from filtered deionized Milli-Q water (Millipore, 18 MΩ·cm). Tips were characterized electrochemically with a Bioanalytical Systems 100W potentiostat equipped with a low-current module while the cell was kept in a grounded Faraday cage. Tapping-mode AFM and a modified SECPM with Nanoscope IIIa controller (from Veeco Instruments) were used.

Results and Discussion

Behavior at a Metallic Electrode Surface. Once a stable well-insulated Ag-covered PtIr probe could be obtained reproducibly, it was used to monitor the potential profile over a Pt foil surface held at different potentials with respect to a stable reference in a dilute KCl solution in the SECPM setup.

An LDPE-coated insulated probe was first opened in the KCl solution in the tunneling mode, and Ag was then electrodeposited ex situ at −300 mV vs PtPPy. The Teflon electrochemical cell was carefully rinsed with purified water between each step. The probes were then immediately used in the STM/SECPM setup to minimize the formation of surface oxides that could affect the behavior of the tip.

Upon successful Ag deposition, the Pt foil surface was approached to tunneling distance (setpoint current, −300 pA) in 10^{-5} M KCl by holding the tip at −400 mV vs PtPPy to prevent AgCl formation while the surface was kept at +500 mV vs PtPPy (surface current ≤25 nA). Once a stable current flowed, the tip was withdrawn 20 μm from the surface and the system was switched into the potentiometric SECPM mode. At this point various approach curves at 20, 60, or 100 nm/s were recorded while the Pt foil surface was kept at different values (400, 300, or 200 mV with respect to PtPPy). The KCl electrolyte concentration was also progressively increased to 10^{-4} and then 10^{-3} M.

Figure 5a shows the normalized potential profile as a function of the Pt foil surface potential in a 10^{-5} M KCl solution. No dependence on the surface potential for values ranging from 200 to 500 mV could be observed as all approach curves overlap perfectly. This is not in agreement with the Gouy−Chapman model for metallic electrodes and could arise from the non-Boltzmannian ion distribution in the SECPM nanogap. On the contrary, changing the electrolyte concentration resulted in the change of the decay length of the obtained potential−distance curves (Figure 5b). The change from 10^{-4} to 10^{-3} M KCl is less pronounced because the expected double layer size of a 1−1 electrolyte at 1 mM (9.6 nm) ceases to be larger than the typical extension of the Pt−Ag nanoprobe used, which is an important source of error when probing the electrical double layer. Since there was no significant difference between the typical potential profile in a 1 and a 0.1 mM KCl solution, where the expected Debye length increases from 9.6 to 30 nm, the tip extension along the probed z-axis is at least 10 nm, i.e., the smallest Debye length for which the tip can still discriminate the double layer from a more concentrated solution.

The advantage of PtIr−Ag electrodes over PtIr or PtIr−Hg electrodes was clearly visible by monitoring the change of the tip potential vs the reference electrode over time when it was held more than 500 μm from the surface. A maximum drift of only 5 mV over 10 min was observed. Moreover, the tip potential far from the surface was within 8 mV of +32 mV vs PtPPy for every PtIr−Ag nanoprobe prepared, whereas the potential of a PtIr probe in a 10 μM KCl or KF solution would be significantly different for each different tip prepared. The stability of the Pt−Ag/KCl system for potentiometry was, therefore, clearly an improvement over Pt tips. The potential of the PtIr−Ag tip is equal to about 0.3 V vs NHE when the PtPPy reference was calibrated by performing CV of a 1 mM solution of $Ru(NH_3)_6Cl_3$ in 0.1 M KCl. A bulk Ag/AgCl electrode in 10^{-5} M chloride ion should be about 0.52 V vs NHE. This is consistent with a lower activity of AgCl on the Ag film, since it was not anodized before use. The tip potential 200 nm from the surface at the initial point of the approach
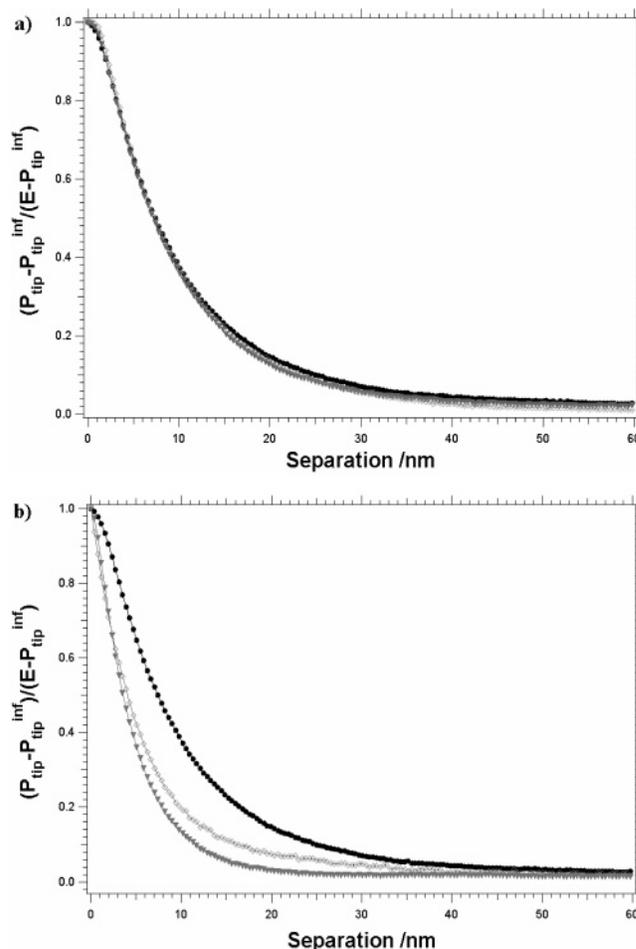
Figure 5. (a) Potentiometric approach curves on the Pt foil surface held respectively at +400 mV (filled black circles), +300 mV (filled gray triangles), and +200 mV vs PtPPy (empty gray boxes) recorded at 20 nm/s in 10 μM KCl. (b) Influence of the electrolyte concentration on the double-layer profile obtained by approaching the Pt foil surface held at +400 mV vs PtPPy at 20 nm/s in 10 μM (filled black circles), 100 μM (filled gray triangles), and 1 mM (empty gray boxes) KCl. The curve corresponding to 1 mM KCl should decay faster than all others. However, in this case the typical electrode size falls within the value of the expected Debye length for a 1−1 electrolyte at 1 mM (9.6 nm). The curves are normalized with the applied surface potential, E, and the tip potential far away from the Pt foil surface, $P_{tip}^{inf} \approx 32$ mV vs PtPPy, for clarity.

curves was less stable than that 500 μm from the surface as can be seen in Figure 6.

A large dependence on the approach speed was also noticed. All curves shown were recorded at 20 nm/s. The difference in the potential profiles for speeds from 20 to 8 nm/s (where the piezoelectric drift starts to be a major problem over 200 nm scans) was found to be negligible; only a 5% change in the decay length was observed. The dependence on approach speed is dictated by the response time of the nanoelectrodes used to probe the Pt foil surface.

The Pt surface could always be approached within 5 mV of the potential applied to the Pt surface (a software limitation to prevent tip crashing), which suggests that the PtIr−Ag tip can probe the surface potential without potential shifts arising from resistance drops and overpotential resulting from current flow into the high input impedance of the measuring system. In this SECPM, the leakage current of the potential measuring circuit is about 3 fA according to the manufacturer's specifications.

After these scans, the tip was again immersed in a 1 M H_2-SO$_4$ solution to record a voltammogram at 1.4 V/s. It showed

Electrochemical Potential Microscopy

J. Phys. Chem. C, Vol. 111, No. 12, 2007 **4625**
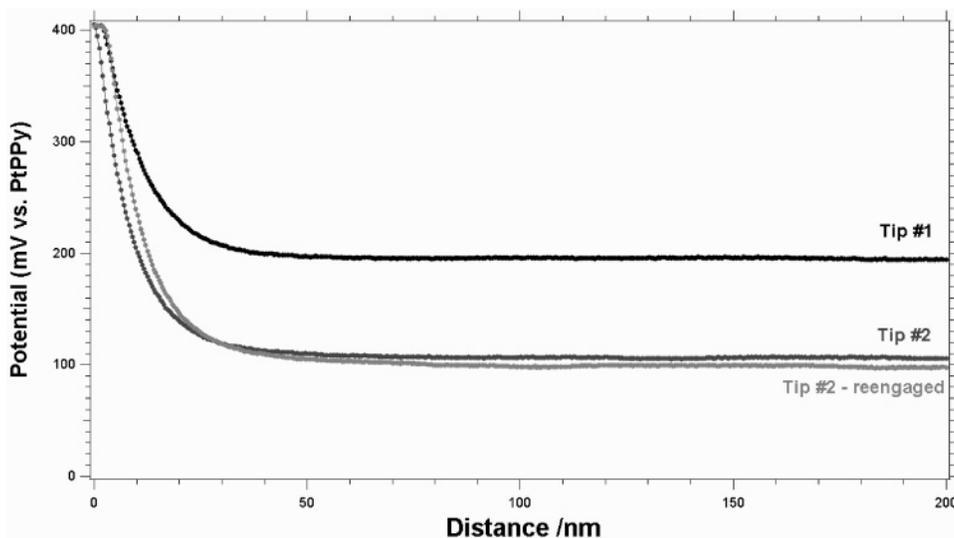
Figure 6. Reproducibility of the SECPM approach curves recorded for three different data sets with two different PtIr−Ag probes in a 10 μM KCl solution. The Pt foil surface is held at +400 mV vs a PtPPy reference electrode.

a large anodic stripping peak around −100 mV vs PtPPy attributed to Ag stripping and no hydrogen adsorption/desorption peaks, suggesting the Pt tip was well covered with Ag throughout the set of SECPM experiments.

Behavior at the Si/SiO$_2$ System. A 1 cm^2 piece of n-Si-(100) wafer was ultrasonicated in MeOH for 15 min, immersed in a 5:1:1 H$_2$O/NH$_4$OH/H$_2$O$_2$ solution heated to 80 °C for 35 min, and immersed in concentrated (49% (v/v)) HF for 20 min. The now hydrophobic piece of Si was immediately inserted into the SECPM Teflon cell so that it could be approached in a tunneling experiment while the tip was held at −400 mV with respect to the reference electrode and the Si surface was held at +50 mV (surface current ∼50 nA). A resistance of about 100 kΩ was measured with a multimeter between the stainless-steel bottom of the Teflon cell where the surface potential was applied and the Si surface in contact with the solution. However, because of the small surface currents used here, this should not affect the surface potential. Once a stable current of about −300 pA flowed, the tip was withdrawn 20 μm from the surface.

Cyclic voltammetry studies showed that passivation of a n-doped Si(100) surface (as determined from the photocurrent obtained when the sample was exposed to a light source) to, for instance, 1 mM ferrocenemethanol oxidation, could be obtained by holding a freshly HF-treated Si(100) sample at +2 V vs PtPPy for 500 s in an air-saturated 100 μM KCl or HCl solution while the cell was illuminated with a flashlight. This treatment produces an insulating oxide film and prevents electron transfer from the surface to the solution. The surface charge of an anodized Si(100) sample is determined by the density and the protonation state of surface silanol groups. The pK_a of two types of silanols, (SiO)$_3$−SiOH and (SiO)$_2$−Si(OH)$_2$, have been estimated at 4.5 and 8.5, respectively, by second-harmonic generation spectroscopy.[32] Therefore, the overall surface charge of the SiO$_2$ surface should be slightly negative. This would establish a Cl$^-$ gradient in the surface double layer with lower concentrations than in the bulk solution. However, applying a high positive potential to the surface results in a positive charge on the surface, given the expected resistive potential drop across the oxide layer. At this point, a capacitive voltammogram was recorded in the 100 μM HCl solution to ensure successful formation of a thick oxide layer on the surface. Then the system was again switched to the potentiometric mode and a potential of +800 mV vs PtPPy was applied to the surface,

before the tip approached the surface. The potential profile was then recorded at an approach speed of 20 nm/s (Figure 7). The anodized Si(100) surface could not be approached in the tunneling mode without crashing the tip. This clearly shows the advantage of SECPM compared with EC-STM and other current-based techniques, since it is not limited to the study of conductive surfaces. Again, the tip was checked for the presence of Ag after the set of approach curves by recording a voltammogram in 1 M H$_2$SO$_4$.

Quantitative Approach. To our knowledge, the theory for a SECPM tip at open circuit attached to a high impedance amplifier and approaching a metallic electrode held at a fixed potential has not been published. It differs from the problem of double-layer overlapping between two charged plates separated by a distance around or below the Debye length for the considered electrolyte—whether the fixed Galvani potential on each plate is identical[33] or different[3] and with the same sign[34]—insofar as the potential boundary condition at the tip is replaced by an electroneutrality condition; i.e., at each distance of the nanogap between the tip and the surface, the total charge on the exposed tip area must be equal and opposite to the total charge in the nanogap.

In the SECPM experiments presented here, the decay length of the potential profile was always smaller than the Debye length from the Gouy−Chapman−Stern theory, which suggests that, as in a previous report,[13] the tip perturbs the potential measurement except in the weakly overlapping region, i.e., when the tip and the sample are still far apart. The situation of a nanogap containing ions has to be considered instead. Kornyshev et al.[3] gave a theoretical description for a nanogap formed between a STM tip and a surface held at fixed potentials. According to the calculations reported, a situation where the potential decay is steeper than that for the linearized Poisson−Boltzmann equation (Gouy−Chapman model) is seen when effects from lattice-saturation in the gap and ion interaction with their image charges within the electrodes occur. These effects may also be present in the SECPM approach curves presented here, although, as mentioned earlier, the boundary conditions are less severe. A more complete model is needed to properly interpret small effects that may occur during a SECPM experiment.

Another question of fundamental interest in SECPM is the response time of the tips used. Feldberg has treated the case of coulostatic charge injection at a metallic electrode from its point
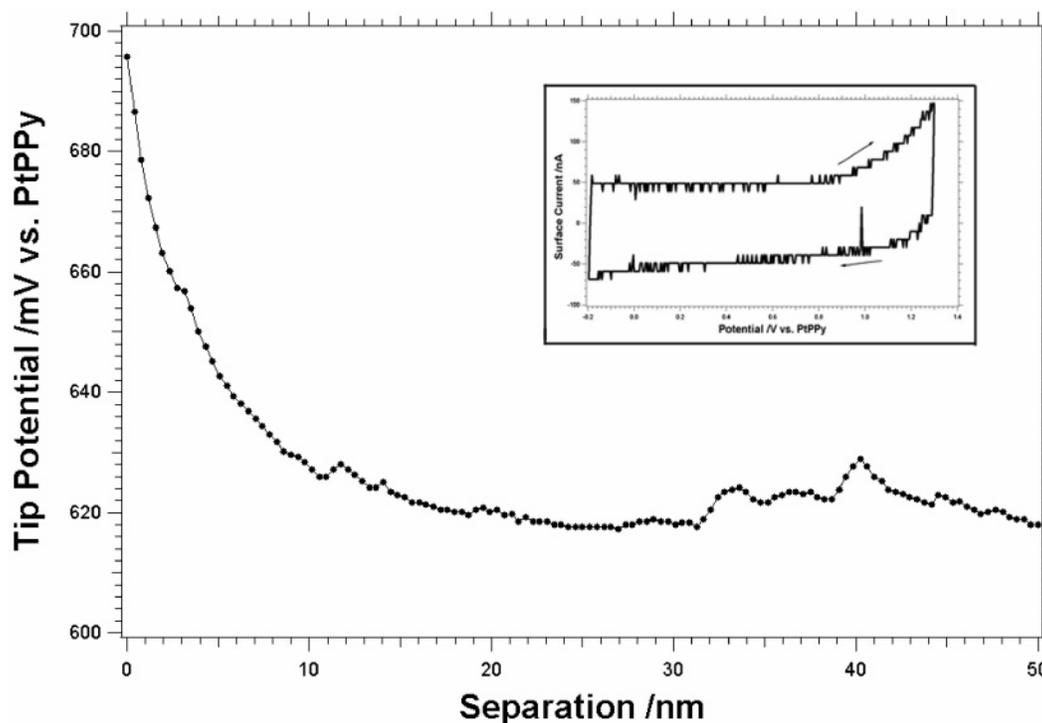
Figure 7. Typical approach curve recorded at 20 nm/s after anodization of the Si−H surface held at +800 mV vs PtPPy in 100 μM HCl. The noise is interpreted as a result of the roughness of the electrochemically grown SiO_2 oxide. The inset shows the capacitive surface voltammogram of the surface after anodization in the HCl solution.
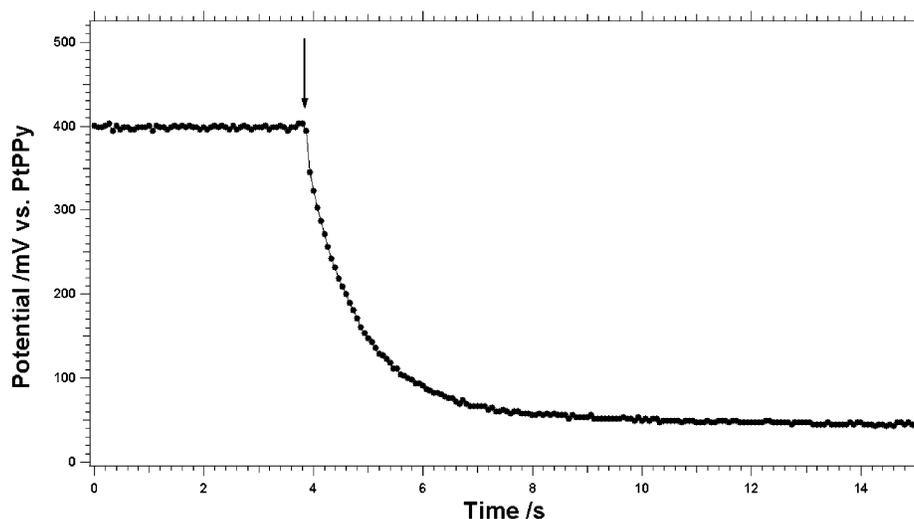
Figure 8. Evolution of the tip potential when a motor step, materialized by the arrow, moves it from within the double layer at a Pt foil held at 400 mV vs PtPPy in 10 μM KCl to a position 20 μm away from the surface. The potential relaxes back to its initial value, $P_{tip}^{\infty} = 32$ mV, after about 5 s. This situation corresponds to the application of a Cl^- concentration step to a metallic Ag electrode held at open circuit.

of zero charge to an applied potential in a 1−1 electrolyte.[35] If his expressions are used in the case of a 10 μM KCl solution, the relaxation time of the double layers at such electrodes is around 30 μs, i.e., faster than the approach speed of 20 nm/s over 200 nm used in the SECPM experiments presented here. However, the situation of SECPM is quite different. A more relevant observation occurs when monitoring how the tip potential returns to the initial value far from the surface, P_{tip}^{∞}, when a fast motor step moves the tip from within the double layer, where Cl^- ions are in excess, to a position 20 μm away where Cl^- ions are at the bulk concentration. It typically took about 5 s for the tip to recover the initial P_{tip}^{∞} potential (Figure 8).

Our data do not fit the Gouy−Chapman−Stern theory. In particular, no dependence on the surface potential over a range from 100 to 500 mV could be observed. Nevertheless, increasing the electrolyte concentration or changing the solvent to methanol, whose relative dielectric constant is lower than that of water, resulted in a change in the decay length of the observed potential profile. This suggests that the assumption that the tip does not perturb the surface double layer and simply reports the surface potential is inaccurate. Indeed, a more complicated situation of a nanogap between the tip and the surface with interacting double layers has to be considered. In this situation, complex effects like ion exclusion and specific adsorption of Cl^- onto

Electrochemical Potential Microscopy

J. Phys. Chem. C, Vol. 111, No. 12, 2007 **4627**

the surface make the ion distribution within the gap deviate from the usually assumed Boltzmann distribution.

Conclusion

We report the use of scanning electrochemical potential microscopy (SECPM) to present an experimental study of electrical double layer profiles on a conductive metallic Pt electrode as well as on an insulating Si/SiO_2 surface. In the latter case, a potentiometric technique like SECPM has an advantage over traditional current-sensing scanning probe methods, as the Si/SiO_2 surface can still be engaged potentiometrically while the tip crashes into the anodized surface in the tunneling mode. The classical Gouy−Chapman−Stern model failed to describe the reported experiments, suggesting that a theoretical treatment taking into account the boundary conditions encountered in SECPM (interaction of double layers between a substrate with a fixed surface potential and a tip at essentially open circuit) is needed to interpret the ion effects in the nanogap formed by the probe and the measured potential profiles.

SECPM could be a unique technique for imaging charge distributions near conducting and insulating surfaces in solution, perhaps down to the atomic level, but tip fabrication and obtaining suitably stable and reproducible tip potentials remain significant problems.

References and Notes

(1) Ren, C. L.; Hu, Y.; Li, D.; Werner, C. *J. Adhes.* **2004**, *80*, 831−849.

(2) Chen, Z.; Singh, R. J. *J. Colloid Interface Sci.* **2002**, *245*, 301−306.

(3) Kornyshev, A. A.; Kuznetsov, A. M. *Electrochem. Commun.* **2006**, *8*, 679−682.

(4) Delgado, A. V.; Arroyo, F. J. *Surfactant Sci. Ser.* **2002**, *106*, 1−54.

(5) Binnig, G.; Rohrer, H.; Gerber, Ch.; Weibel, E. *Phys. Rev. Lett.* **1982**, *49*, 57−61.

(6) Hillier, A. C.; Kim, S.; Bard, A. J. *J. Phys. Chem.* **1996**, *100*, 18808−18817.

(7) Hu, K.; Chai, Z.; Whitesell, J. K.; Bard, A. J. *Langmuir* **1999**, *15*, 3343−3347.

(8) Lee, I.; Greenbaum, E.; Budy, S.; Hillebrecht, J. R.; Birge, R. R.; Stuart, J. A. *J. Phys. Chem. B* **2006**, *110*, 10982−10990.

(9) Israelachvili, J. N. *Intermolecular and Surfaces Forces*, 2nd ed.; Academic Press: London, 1992.

(10) O'Reilly, J. P.; Butts, C. P.; l'Anson, I. A.; Shaw, A. M. *J. Am. Chem. Soc.* **2005**, *127*, 1632−1633.

(11) Nonnenmacher, M.; O'Boyle, M. P.; Wickramasinghe, H. K. *Appl. Phys. Lett.* **1991**, *58*, 2921−2923.

(12) Viswanathan, R.; Heanye, M. B. *Phys. Rev. Lett.* **1995**, *75*, 4433−4436.

(13) Woo, D.-R.; Yoo, J.-S.; Park, S.-M.; Jeon, I. C.; Kang, H. *Bull. Korean Chem. Soc.* **2004**, *25*, 577−580.

(14) Parsons, R. *Chem. Rev.* **1990**, *90*, 813−826.

(15) Delahay, P. *Double Layer and Electrode Kinetics*; John Wiley & Sons: New York, 1965.

(16) Spitzer, J. J. *Nature* **1984**, *310*, 396−397.

(17) Duval, J. F. L.; Leermakers, F. A. M.; van Leeuwen, H. P. *Langmuir* **2004**, *20*, 5052−5065.

(18) Chuarev, N. V. *Adv. Colloid Interface Sci.* **2003**, *103*, 197−218.

(19) Forcada, J.; Hidalgo-Alvarez, R. *Curr. Org. Chem.* **2005**, *9*, 1067−1084.

(20) de Young, L. R.; Fink, A. L.; Dill, K. A. *Acc. Chem. Res.* **1993**, *26*, 614−620.

(21) Li, C.; Kjoller, K. Abstract 1360 of the 201st Meeting of the Electrochemical Society, Philadelphia, PA, 2002.

(22) Gewirth, A. A.; Craston, D. H.; Bard, A. J. *J. Electroanal. Chem.* **1989**, *261*, 477−482.

(23) Nagahara, L. A.; Thundat, T.; Lindsay, S. M. *Rev. Sci. Instrum.* **1989**, *60*, 3128−3130.

(24) Fan, F.-R. F.; Kwak, J.; Bard, A. J. *J. Am. Chem. Soc.* **1996**, *118*, 9669−9675.

(25) Ghilane, J.; Hapiot, P.; Bard, A. J. *Anal. Chem.* **2006**, *78*, 6868−6872.

(26) Grahame, D. C.; Soderberg, B. A. *J. Chem. Phys.* **1954**, *22*, 449−460.

(27) Hameln, A.; Borkowska, Z.; Stafiej, J. *J. Electroanal Chem.* **1989**, *269*, 191−195.

(28) Wehmeyer, K. R.; Wightman, R. M. *Anal. Chem.* **1985**, *57*, 1989−1993.

(29) (a) Gunawardena, G.; Hills, G. J.; Montenoegro, I. *Electrochim. Acta* **1978**, *23*, 693−697. (b) Gunawardena, G.; Hills, G. J.; Sharifker, B. *J. Electroanal. Chem.* **1981**, *130*, 99−112.

(30) Durney, L. J. *Electroplating Engineering Handbook*, 4th ed.; Van Nostrand Reinhold: New York, 1984.

(31) Ives, D. J. G.; Janz, G. J. *Reference Electrodes*; Academic Press: New York, 1961.

(32) Ong, S.; Zhao, X.; Eisenthal, K. B. *Chem. Phys. Lett.* **1992**, *191*, 327−335.

(33) Shi-Min, Z. *Surf. Rev. Lett.* **2004**, *11*, 311−320.

(34) Zhang, Y.; Jin, J.; Luo, G.; Wang, H. *Colloid Polym. Sci.* **2003**, *281*, 401−406.

(35) Feldberg, S. W. *J. Phys. Chem.* **1970**, *74*, 87−90.